Sensitive SERS-pH Sensing in Biological Media Using Metal Carbonyl Functionalized Planar Substrates

Kong Kien Voon[a], Dinish U. S[a], Weber Lau[b], Malini Olivo*[, a, c, d]

[a] Bio-Optical Imaging Group, Singapore Bioimaging Consortium,
Agency for Science Technology and Research (A*STAR),
11 Biopolis Way, Singapore 138667
[b] Department of Urology, Singapore General Hospital, Singapore
[c] School of Physics, National University of Ireland Galway, Galway, Ireland
[d] Department of Pharmacy, Faculty of Science, National University of Singapore,
18 Science Drive 4, Singapore 117543

* Corresponding author:
Prof. Malini Olivo
E-mail: Malini_Olivo@sbic.a-star.edu.sg

Abstract

Conventional nanoparticle based Surface enhanced Raman scattering (SERS) technique for pH sensing often fails due to the aggregation of particles when detecting in acidic medium or biosamples having high ionic strength. Here, We develop SERS based pH sensing using a novel Raman reporter, arene chromium tricarbonyl linked aminothiophenol ($Cr(CO)_3$)-ATP), functionalized onto a nano-roughened planar substrates coated with gold. Unlike the SERS spectrum of the ATP molecule that dominates in the 400 –1700 cm^{-1} region, which is highly interfered by bio-molecules signals, metal carbonyl-ATP ($Cr(CO)_3$)-ATP) offers the advantage of monitoring the pH dependent strong CO stretching vibrations in the mid-IR (1800-2200 cm^{-1}) range. Raman signal of the CO stretching vibrations at ~1820cm^{-1} has strong dependency on the pH value of the environment, where its peak undergo noticeable shift as the pH of the medium is varied from 3.0 to 9.0. The sensor showed better sensitivity in the acidic range of the pH. We also demonstrate the pH sensing in a urine sample, which has high ionic strength and our data closely correlate to the value obtained from conventional sensor. In future, this study may lead to a sensitive chip based pH sensing platform in bio-fluids for the early diagnosis of diseases.

Key Words: Surface enhanced Raman scattering, pH sensing, metal carbonyl reporter molecule, SERS substrates, urine sample

1. Introduction

Enhancement of weak Raman scattering is achieved in surface enhanced Raman scattering (SERS) when analyte molecules are brought into the close proximity (in nanometric scale) of a nano-roughened metal substrates or noble metal colloids such as silver (Ag) or gold (Au) (Albrecht et al., 1977; Dinish et al., 2011; Jeanmaire et al., 1977; Ko et al., 2008; Moskovits, 2005). Recently, SERS has been emerged as a powerful analytical tool for various molecular and cellular sensing/imaging applications. This is achieved primarily due to the tremendously high sensitivity (even up to single molecule detection) that it can offer and also the ability to generate unique 'fingerprint' Raman spectra of different molecules, which makes it possible to track the targeted molecule in complex biological conditions (Kho et al., 2011; Kneipp et al., 2008; Zhang et al., 2011). SERS is being developed as clinical tool for the detection of various biomarkers that facilitates the early detection of diseases and offers great sensitivity for the detection of cells (Kong et al., 2012) and various bio-molecules such as proteins (Han et al., 2009; Jehn et al., 2009), peptides (Herne et al., 1991; Stewart et al., 1999), and bacteria (Efrima et al., 1998; Yang et al., 2011).

Recently, biological pH sensing based on SERS has generated great interest. Such a pH sensor is realised by covalently anchoring a strong Raman active molecule (Reporter molecule, RM) onto Ag and Au nanoparticles (NPs) and monitor the changes in SERS signal of the RM as a function of the pH of the surrounding environment (Ando et al., 2009; Kneipp et al., 2007; Lim et al., 2006; Nowak-Lovato et al., 2009; Pallaoro et al., 2010; Talley et al., 2004; Wang et al., 2008; Zhao et al., 2008; Zong et al., 2011). Zong *et al* developed pH sensor using hydrochloric acid treated Au nanorods. These nanorods, unlike conventional cetyltrimethylammonium bromide (CTAB) stabilized nanoords that are toxic, showed improved SERS sensitivity and reduced cytotoxicity due to the removal of CTAB molecules (Zong et al., 2011). In an another interesting design to interrogate the intracellular pH, SERS active tips are created on the tip of a multimode fiber by Ag coating followed by attaching the pH responsive RM (Scaffidi et al., 2009).

Three most commonly used pH responsive RMs are 4-mercaptobenzoic acid (4MBA), 2-aminothiophenol (2ATP) and p-aminothiophenol (pATP), which is an isomer of 2ATP (Zong et al., 2011). It was reported that the carboxyl groups of 4MBA exhibit the COO^- form in alkaline solutions leading to a higher sensitivity in the alkaline region (Talley et al., 2004) where as the amino group in the 2ATP exhibit the $NH3^+$ form in acidic solutions to provide a better sensitivity in the acidic range (Wang et al., 2008). pH response for the SERS peak of pATP was originated from the transformation between two states, i.e. the aromatic state in acidic solutions and the quinonoidic form in neutral and alkaline medium (Hill et al., 1993).

Though SERS based pH sensing using above mentioned molecules has lot of potential, but it is associated with some serious shortcomings. SERS spectrum of these organic RMs is dominated in the 400–1700 cm^{-1} region, which can be highly interfered by the signals from bio-molecules. This crowded window of the Raman signal often limits its application for pH sensing in a complex environments. Moreover, due to the aggregation of NPs, reported metal colloidal particle based pH sensing often fails in a medium having high ionic strength such as urine (Kho et al., 2008). Moreover, SERS signal from such a nano-construct often fluctuates in a strongly acidic medium.

In this context, we demonstrate the pH sensing using a metal carbonyl modified ATP as a reporter molecule anchored onto a planar SERS substrate fabricated by the optimized bimetallic (Au on top of Ag) coating on top of the polystyrene nanosphere immobilized onto the base glass material. One of the useful characteristics of using metal carbonyl compounds is the strong CO stretching vibrations in the mid-IR (1800-2200 cm^{-1}); a region which is relatively free of interference from absorbance of bio-molecules (Kong et al., 2007; Salmain et al., 1993; Vessieres et al., 1988). Here, we introduce a metal carbonyl fragment ($Cr(CO)_3$) to ATP molecule to form the new reporter molecule, where aromatic ring of ATP can act as a six-electron donor to $Cr(CO)_3$ to form $Cr(CO)_3$ conjugated ATP-(($Cr(CO)_3$)-ATP). Protonation and deprotonation of the pH responsive NH_2 group in the ATP can induce electronic changes within the aromatic ring and $Cr(CO)_3$, which reflects in the CO stretching vibrations. As a result, SERS signal of the CO vibration (~1820 cm^{-1}) changes as a function of the pH of the medium is varied from 3 to 9. As a proof-of-concept, we also successfully demonstrate the pH sensing in a urine sample, which has a high ionic strength and our data closely correlate to the value obtained from conventional pH sensor. To the best of our knowledge, this is the first demonstration of the SERS-pH sensing using a planar substrate. We believe that in future, this study may lead to a sensitive chip based pH sensing platform for the early diagnosis of diseases in bio-fluids.

2. Materials and Methods

2.1 Fabrication of SERS Substrates

Clean standard microscope glass slides pieces are used as supporting base material for the fabrication of substrates. Initially, glass slides were sonicated in a bath of ethanol for 20 minutes before being dried with argon gas. Subsequently, mono-disperse polystyrene (PS) NPs (Kisker, Ø = 384 nm, 2.5 wt%) solution was mixed with 15wt% surfactant, sodium dodecyl sulphate (SDS), to form a composite solution and spin coated (Cee 200X, Brewer Science, USA) onto the cleaned glass pieces (Fu et al., 2012). PS beads are closely packed in a hexagonal arrangement. These coated glass slides were then dried in vacuum desiccators at 0.6 pa pressures overnight. Later, these substrates were first coated with 120 nm Ag (99.999% purity, JEOL) and then 80 nm Au (99.999% purity, JEOL) using

sputtering (JEOL JFC-1600 Auto fine coater) machine. Scanning electron microscopy (SEM, JEOL, SEM 6340F) of the substrates was used to examine the surface morphology of the bimetallic substrates, especially at the SERS-active regions where PS beads are closely packed.

2.2 Preparation of Raman Reporter and Immobilization onto SERS Substrate

All manipulations for chemical synthesis were carried out using standard Schlenk techniques under an argon or nitrogen atmosphere. The $Cr(CO)_3$-ATP, was prepared according to the reported procedure (Anson et al., 1996). Initially, p-Aminothiophenol (sigma-aldrich) was dissolved in ethanol to attain 10 mM solution. Later, fabricated SERS substrates were then incubated with the prepared p-ATP solution for 2 hrs. Substrates were then washed thoroughly with pure ethanol and dried in Argon. Subsequently, ATP immobilized substrates and $Cr(CO)_6$ (sigma-aldrich 10 mM) were heated at 60 ^oC in dibutyl ether (sigma-aldrich, 30 mL) for 6 hrs (schematic in Supporting Information (SI), Fig. S1). Finally, substrates were washed with dibutyl ether and dried under argon flow. For sensing, 20 µL of the respective solutions (pH 3 to 11) were added to the functionalized substrate and incubated for 15 minutes before SERS measurement was carried out.

2.3 Detection of pH in the acidified clinical urine sample

In this experiment, samples used for the study were from clinical specimens, stored at −20°C. Specimens were used in accordance to procedures with approval of the local ethics committee (CIRB Re 2011/558/C, Singapore General Hospital) and informed consent was given by all patients. Urine sample was acidified with 10% HCl solution. The pH of urine may range from 4.5 to 8, depending on the person's acid-base status. The urinary pH was adjusted to pH 5.2 and 5.8 as confirmed by bench top pH meter (Thermo Scientific). The final urine solution was mixed thoroughly upon substrate incubation. SERS spectral acquisition was carried out after 5 minutes of incubation and all the measurements were carried out in triplicate.

2.4 SERS Measurements

The SERS measurements were carried out using a Renishaw InVia Raman (UK) microscope with 633 nm laser and equipped with a grating (1800 line/mm, spectral resolution at 0.7 cm^{-1}) and a CCD detector cooled at -70°C. The laser beam is directed to the sample through a 50× objective lens and same lens was also used to collect the return Raman signal. All SERS spectra were processed with WiRE 3.2 software. The maximum laser power at the sample was measured to be 0.6mW and the

exposure time was set at 10s throughout the measurements. Prior to each measurement, the instrument was calibrated with a silicon standard whose Raman peak is cantered at 520 cm^{-1}.

3. Results and Discussion

3.1 Morphological Characterization of Substrates and SERS Mapping

SEM of the SERS-active PS beads arrays with Ag under layer and Au over layer showed the formation of large area of hexagonally-packed two dimensional colloidal crystals due to the self-assembly of particles (Fig. 1A). The nano-roughness required for the plasmonic coupling is primarily contributed by the roughness created by the metal coating as well as the undulations on the metal layer due to the underlying periodic nanostructures. Higher metal thickness helped to reduce the inter-bead gaps and forms a uniform structure (Fu et al., 2012). This will lead to high SERS enhancement and as well as reduced point to point intensity variation. At the optimized metal coating, the inter-bead gap is only ~ 20nm. The morphology study suggests that the SERS enhancement is originates from the hot-spots distributed primarily at the junctions of interconnected PS beads as well as over the surface of beads with Au and Ag layers.

We optimized the metal thickness to achieve highest SERS enhancement and stability for substrates. Though Ag layer can produce highest SERS enhancement, but it is susceptible for oxidation. Moreover, Ag layer often gets peeled off when testing with biological samples in phosphate buffer saline (Scholes et al., 2008). Moreover, laser-induced structural changes in the silver oxide layers can cause fluctuating SERS intensity (Buchel et al., 2001). In our case, the upper Au layer is relatively inert and hence protects the underlying Ag and also provides a sufficient SERS enhancement. If the thickness of the upper Au layer is further increased, it may lead to smoothening of crevices between the beads and will eventually limits the SERS sensitivity.

p-ATP has a strong pH-sensitive amine group and it can covalently attach onto the bimetallic substrates to form a monolayer through the interaction between thiol group and Au layer. Moreover, ATP has an arene group, which is an ideal functional group for the incorporation of the $Cr(CO)_3$ unit. Initially, we attempted to do pH sensing using $Cr(CO)_3$)-ATP immobilized onto 60 nm AuNPs. We observed that NPs undergo aggregation with increase in ATP concentration. Further, when urine sample is added to $Cr(CO)_3$)-ATP immobilized AuNPs, severe aggregation is occurred due to the high ionic strength of the sample. TEM images and absorbance spectra confirms the aggregation of the particles (Fig. S2, SI). It is evident that the absorbance spectrum of the NPs gets red shifted at higher aggregation. This study confirms the limitations of the NP based pH sensing using SERS.

As a means of a versatile system implementation, we carried out the pH sensing using planar SERS substrates. Un-enhanced Raman spectrum of ATP on glass slide, SERS spectrum of ATP and $Cr(CO)_3$)-ATP on BMFON substrate at various laser power are provided in Fig. S3 (in SI). SERS spectrum of p-ATP molecule before and after incorporation of $Cr(CO)_3$ and immobilized onto the substrates is shown in Fig. 1B. In this case, the obvious site for incorporation of Cr $(CO)_3$ unit to p-ATP is the six-electron donor, arene group. Two CO signals at 1820 cm^{-1} and 1910 cm^{-1} were observed in SERS spectrum after the incorporation of $Cr(CO)_3$ unit, which is similar to reported value (Adams et al., 1970). The appearance of CO signals in the SERS spectrum is attributed to the $Cr(CO)_3$ incorporation to ATP. An additional arene peak at 1610 cm-1 suggests that the attachment of $Cr(CO)_3$ to ATP is *via* η6-bond formation.

To understand the relative distribution of reporter molecules onto substrates, we carried out SERS mapping before and after incorporating $Cr(CO)_3$ group onto p-ATP immobilised substrates (Fig. 1C). The distribution of ATP molecule prior to the incorporation of $Cr(CO)_3$ was examined by SERS mapping of Raman peak originated from arene group (1580 cm^{-1}). This mapping result confirms that p-ATP molecules are distributed uniformly and a monolayer is formed onto the SERS substrate. After the incorporation of metal carbonyl units to the ATP, we further carried out SERS mapping of CO peak (~1820cm^{-1}) and results confirmed that the addition of $Cr(CO)_3$ did not alter the distribution of the molecules on the substrate.

Fig 1 here

3.2 pH sensing using $Cr(CO)_3$-ATP functionalized substrate

The schematic of the immobilization of reporter molecules onto substrate for pH sensing is shown in Fig 2A. As shown in Fig. 2B, we observed an obvious shift in the CO Raman vibrational peak when a small amount of different pH buffer solutions were added to $Cr(CO)_3$-ATP functionalized substrate. Peak at 1820 cm^{-1} was used for the study of pH effect because it has higher intensity than the peak at 1910 cm^{-1}. When acidic solution was used, the Raman peak at ~1820 cm^{-1} showed obvious shift to lower wave number and when the medium become more acidic, the peak moved further left and reaches the limiting values of 1807 cm^{-1} at pH 3. Experiment was repeated three times and average value with error bar is plotted as in Fig 2C. It can be seen that there is an overall decreasing trend for the CO vibration Raman peak when the sensor was exposed from an alkaline to acidic environment. At neutral pH (pH 7), the CO peak showed a Raman shift at ~1818cm^{-1} and it is increased to ~1820 cm^{-1} when pH of the buffer is 10. This plot enables the readout of the pH of the solution from the spectroscopic data. The pK_a of $Cr(CO)_3$-ATP can be estimated from the plot as ca. 6.1. This can be

compared with 6.85, the pKa of pure p-ATP in water. The decrease in pKa upon incorporation by $Cr(CO)_3$ is in line with previous studies (Anson et al., 1996). In $Cr(CO)_3$-ATP, the protonation of the amine substituent would be expected to decrease the electron density on the $Cr(CO)_3$ moiety which in turn decrease the extent of electron back-donation from the metal to the CO CO π^*-antibonding orbitals. In this way, protonation of the complex should lead to a lowering in wave number of the CO modes, an effect that allows the use of this mode to give a spectroscopic readout defining the pH of the solution.

Fig 2 here

3.3 pH Sensing in Clinical Urine Sample

After the successful demonstration of pH sensing using metal carbonyl derived p-ATP on SERS substrates, we further carried out the sensing in a biological environment. Urine pH is one of the physiological parameters commonly measured in clinics. Urine pH is an important screening test for the diagnosis of renal diseases such as renal tubular acidosis (RTA). RTA is a syndrome of accumulation of acid in the body because of the failure of kidneys to appropriately acidify the urine. RTA has been classified into three categories, that are, distal RTA (type 1), proximal RTA (type 2), and hyperkalemic RTA (type 4) (Rodríguez Soriano, 2002; Soriano et al., 1967). Urinary pH is one of the ways to classify type 1 and type 4 RTA. Patients with type 1 are unable to properly lower their urinary pH (>pH 5.5), whereas patients with type 4 are able to lower urine pH below 5.5 by excretion of adequate amounts of NH_2. As a proof-of-concept to demonstrate the potential application of our sensor in bio-fluid, we carried out the pH measurement at two clinically relevant urinary pH values (pH 5.2 and pH 5.8). When first urine sample was introduced into the SERS sensor, the Raman shift of the CO peak was found to be ~1811cm^{-1}, while for the second sample it was 1813.2cm^{-1} as shown in Fig. 3A, We also observed that due to the presence of various bio-molecules inside the urine, the spectral range of 500-1700cm^{-1} is very crowded and monitoring of the Raman peak of pure p-ATP is not reliable for pH sensing. In this context the CO peak ~ 1820cm^{-1} is really useful and offers a sensitive option for the pH sensing. From the observed response curve obtained as in Fig.2B, the pH value corresponds to the 1811cm^{-1} and 1813.2cm^{-1} peak are 5.2 and 5.8 (Fig. 3B). The accuracy of our sensor was established by comparing the observed result with a reference measurement using a calibrated biochemistry laboratory bench top pH meter. Our result was in very close agreement to the bench top pH meter (± 0.2 pH units), which is considered as the gold-standard for urine pH analysis. This study confirms the sensitivity and a clinically relevant application of our SERS sensor for pH sensing with great accuracy.

Fig 3 here

Conclusion

We successfully developed a SERS-pH sensor by using chromium tricarbonyl linked aminothiophenol as RM functionalized onto nano-roughened planar substrate. This new RM offers a platform for pH sensing by monitoring the Raman shift in a spectral range, which is relatively free of the peaks from bio-molecules. The mechanism of pH sensing using $Cr(CO)_3$-ATP is attributed to the protonation and deprotonation of the pH responsive amino group in the ATP that can induce electronic changes within the aromatic ring and $Cr(CO)_3$ and that reflects in the Raman peak of CO stretching vibrations at ~1820cm^{-1}. This sensor exhibited better sensitivity in the acidic pH range of the sample. As a proof-of- concept, we also successfully demonstrate the pH sensing in a clinical urine sample with great accuracy. This is the first demonstration of a planar substrate based pH sensing using SERS and it helps to overcome the limitation of the NP aggregation when working in acidic and as well as sample having high ionic strength. Further, the bimetallic planar substrate that we developed is stable, highly cost effective and easy to fabricate. In future, this study may lead to a sensitive chip based pH sensing platform in bio-fluids and potentially for the early diagnosis of diseases. Currently we are developing an optical fiber based SERS pH sensing for various cellular and biological applications.

Acknowledgement: The authors would like to thank Mr. Ong Chong Jin (Attachment student from Nanyang Technological University, Singapore) for his help in this project.

References

Adams, D.M., Squire, A., 1970. J. Chem. Soc. A, 814-821.

Albrecht, M.G., Creighton, J.A., 1977. J. Am. Chem. Soc. 99, 5215-5217.

Ando, R.A., Pieczonka, N.P.W., Santos, P.S., Aroca, R.F., 2009. Phys. Chem. Chem. Phys. 34, 7505-7508.

Anson, C.E., Baldwin, T.J., Creaser, C.S., Fey, M.A., Stephenson, G.R., 1996. Organometallics 15, 1451-1456.

Buchel, D., Mihalcea, C., Fukaya, T., Atoda, N., Tominaga, J., Kikukawa, T., Fuji, H., 2001. Appl. Phys. Lett. 79, 620-622.

Dinish, U.S., Yaw, F.C., Agarwal, A., Olivo, M., 2011. Biosens. Bioelectron. 26, 1987-1992.

Efrima, S., Bronk, B.V., 1998. J. Phys. Chem. B 102, 5947-5950.

Fu, C.Y., Kho, K.W., Dinish, U.S., Koh, Z.Y., Malini, O., 2012. J. Raman Spectrosc. 43, 977-985.

Han, X.X., Huang, G.G., Zhao, B., Ozaki, Y., 2009. Anal. Chem. 81, 3329-3333.

Herne, T.M., Ahern, A., Garrell, R.L., 1991. J. Am. Chem. Soc. 113, 846-854.

Hill, W., Wehling, B., 1993. J. Phys. Chem. 97, 9451-9455.

Jeanmaire, D.L., Van Duyne, R.P., 1977. J. Electroanal. Chem. Interfacial Electrochem. 84, 1-20.

Jehn, C., Kustner, B., Adam, P., Marx, A., Strobel, P., Schmuck, C., Schlucker, S., 2009. Phys. Chem. Chem. Phys. 11, 7499-7504.

Kho, K.W., Fu, C.Y., Dinish, U.S., Olivo, M., 2011. J. Biophotonics 4, 667-684.

Kho, K.W., Qing, K.Z.M., Shen, Z.X., Ahmad, I.B., Watt, F., Soo, K.C., Olivo, M., Lim, S.S.C., Mhaisalkar, S., White, T.J., 2008. J. Biomed. Opt. 13, 54026-54029.

Kneipp, J., Kneipp, H., Kneipp, K., 2008. Chem. Soc. Rev. 37, 1052-1060.

Kneipp, J., Kneipp, H., Wittig, B., Kneipp, K., 2007. Nano Lett. 7, 2819-2823.

Ko, H., Singamaneni, S., Tsukruk, V.V., 2008. Small 4, 1576-1599.

Kong, K.V., Chew, W., Lim, L.H., Fan, W.Y., Leong, W.K., 2007. Bioconj. Chem. 18, 1370–1374.

Kong, K.V., Lam, Z., Goh, W.D., Leong, W.K., Olivo, M., 2012. Angew. Chem. Int. Ed. 51, 9796-9799.

Lim, J.K., Joo, S.-W., 2006. Appl. Spectrosc. 60, 847-852.

Moskovits, M., 2005. J. Raman Spectrosc. 36, 485-496.

Nowak-Lovato, K.L., Rector, K.D., 2009. Appl. Spectrosc. 63, 387-395.

Pallaoro, A., Braun, G.B., Reich, N.O., Moskovits, M., 2010. Small 6, 618-622.

Rodríguez Soriano, J., 2002. J Am. Soc. Nephrol. 13, 2160-2170.

Salmain, M., Vessieres, A., Brossier, P., Jaouen, G., 1993. Anal. Biochem. 208, 117-120.

Scaffidi, J., Gregas, M., Seewaldt, V., Vo-Dinh, T., 2009. Anal. Bioanal. Chem. 393, 1135-1141.

Scholes, F.H., Bendavid, A., Glenn, F.L., Critchley, M., Davis, T.J., Sexton, B.A., 2008. J. Raman Spectrosc. 39, 673-678.

Soriano, J.R., Boichis, H., Stark, H., Edelmann, C.M., 1967. Pediatr. Res. 1, 81-98.

Stewart, S., Fredericks, P.M., 1999. Spectrochim. Acta Mol. Biomol. Spectros. 55, 1615-1640.

Talley, C.E., Jusinski, L., Hollars, C.W., Lane, S.M., Huser, T., 2004. Anal. Chem. 76, 7064-7068.

Vessieres, A., Top, S., Ismail, A.A., Butler, I.S., Louer, M., Jaouen, G., 1988. Biochemistry 27, 6659-6666.

Wang, Z., Bonoiu, A., Samoc, M., Cui, Y., Prasad, P.N., 2008. Biosens. Bioelectron. 23, 886-891.

Yang, X., Gu, C., Qian, F., Li, Y., Zhang, J.Z., 2011. Anal. Chem. 83, 5888-5894.

Zhang, Y., Hong, H., Myklejord, D.V., Cai, W., 2011. Small 7, 3261-3269.

Zhao, L., Shingaya, Y., Tomimoto, H., Huang, Q., Nakayama, T., 2008. J. Mater. Chem. 18, 4759-4761.

Zong, S., Wang, Z., Yang, J., Cui, Y., 2011. Anal. Chem. 83, 4178-4183.

Figure Captions

Figure 1

(A) SEM image of bimetallic substrate at different magnifications. The inter-bead gap is estimated to be ~20nm.

(B) SERS spectra of pH responsive reporter molecule immobilized onto the substrate. (I) from ATP and (II) from $Cr(CO)_3$-ATP. pH responsive Raman peak of $Cr(CO)_3$-ATP is marked.

(C) Bright field and SERS mapping images. (I) bright field image of the substrate alone, (II) SERS mapping image of the substrate before immobilizing the ATP reporter molecule, (III) SERS mapping image at 1580 cm^{-1} peak of ATP and (IV) SERS mapping image at 1820 cm^{-1} of $Cr(CO)_3$-ATP.

Figure 2

(A) The schematic representation of the immobilization of reporter molecules onto bimetallic SERS substrate for pH sensing and the mechanism of sensing.

(B) Shift in SERS peak at ~1820cm^{-1} of $Cr(CO)_3$-ATP immobilized onto substrates at different pH value of the solutions.

(C) Response curve showing the shift in SERS peak of the CO vibration in $Cr(CO)_3$-ATP at ~1820cm^{-1} as a function of different pH value of the test solutions. Error bars for the three repeated measurements are shown.

Figure 3

(A) SERS spectra of the $Cr(CO)_3$-ATP reporter molecule when acidic urine samples at pH 5.2 and 5.8 are added onto the functionalized substrate. The highly overlapped spectral region due to the interference from bio-molecules in the urine as well as relatively clear region for pH monitoring is marked.

(B) Measured pH value of the urine solution from the response curve.

Figure 1

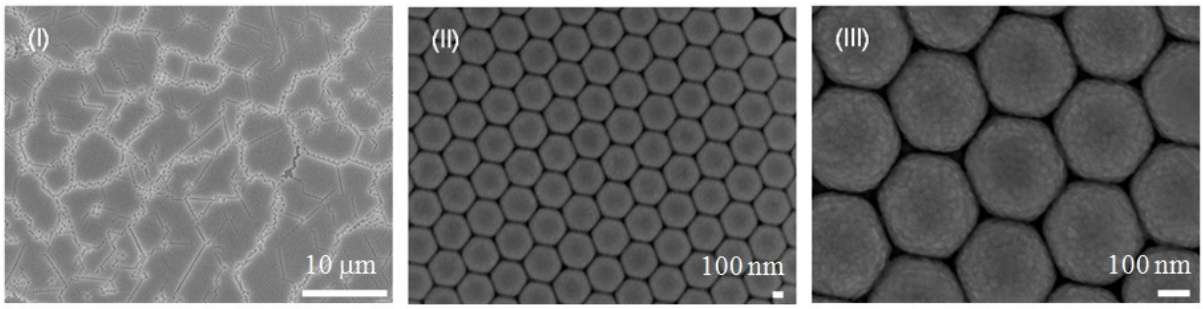
(I)
10 µm
(II)
100 nm
(III)
100 nm

(A)

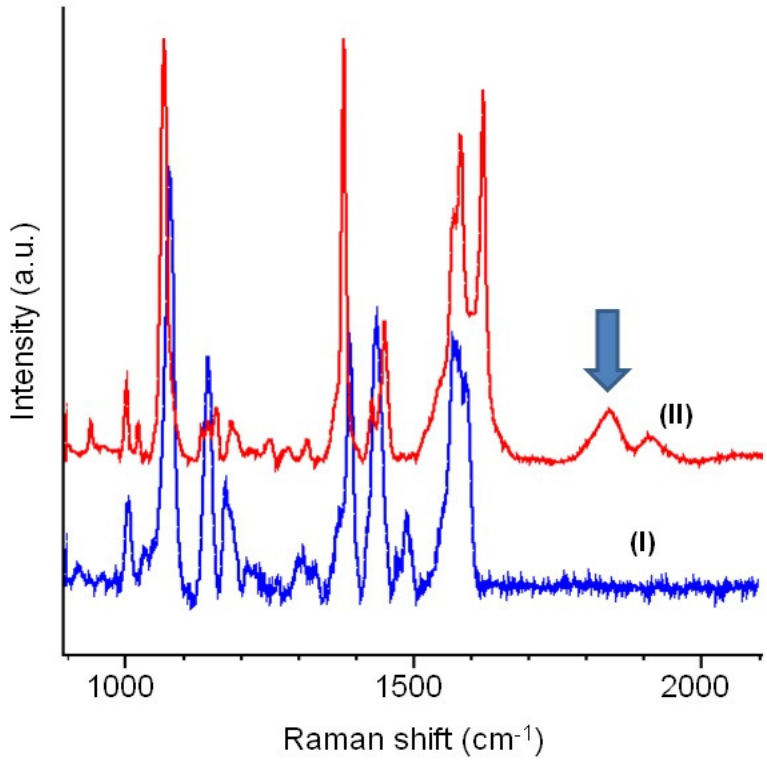
Intensity (a.u.)
(II)
(I)
1000
1500
2000
Raman shift (cm-1)

(B)

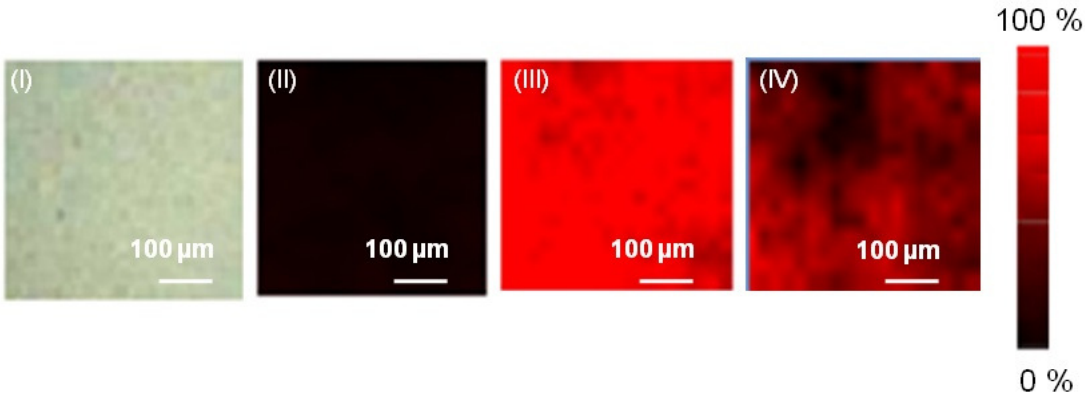
(I)
100 µm
(II)
100 µm
(III)
100 µm
(IV)
100 µm
100 %
0 %

(C)

Figure 2

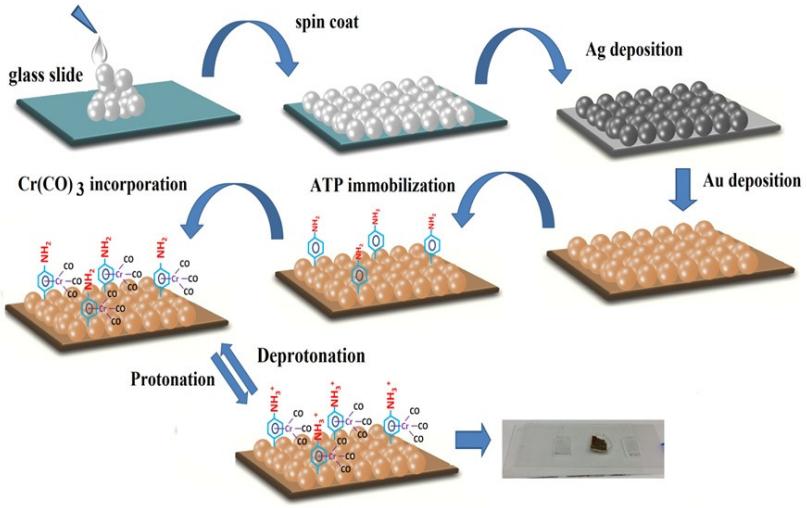
glass slide
spin coat
Ag deposition
Cr(CO) 3 incorporation
ATP immobilization
Au deposition
Deprotonation
Protonation

(A)

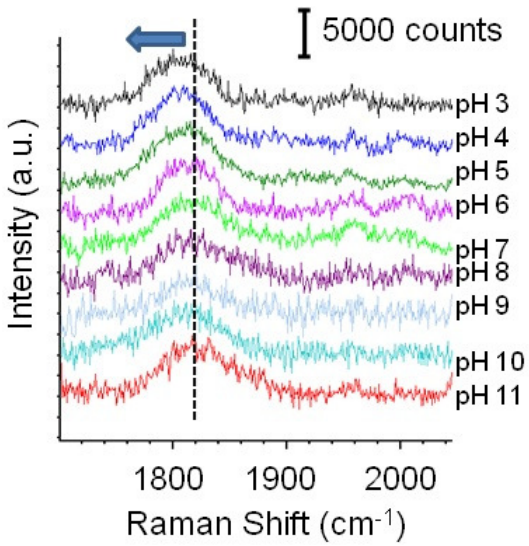
5000 counts
pH 3
pH 4
pH 5
pH 6
pH 7
pH 8
pH 9
pH 10
pH 11
Intensity (a.u.)
1800
1900
2000
Raman Shift (cm-1)

(B)

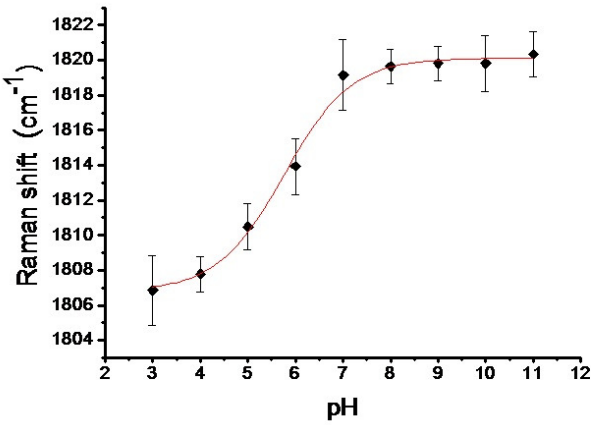
Raman shift (cm-1)
1822
1820
1818
1816
1814
1812
1810
1808
1806
1804
2
3
4
5
6
7
8
9
10
11
12
pH

(C)

Figure 3

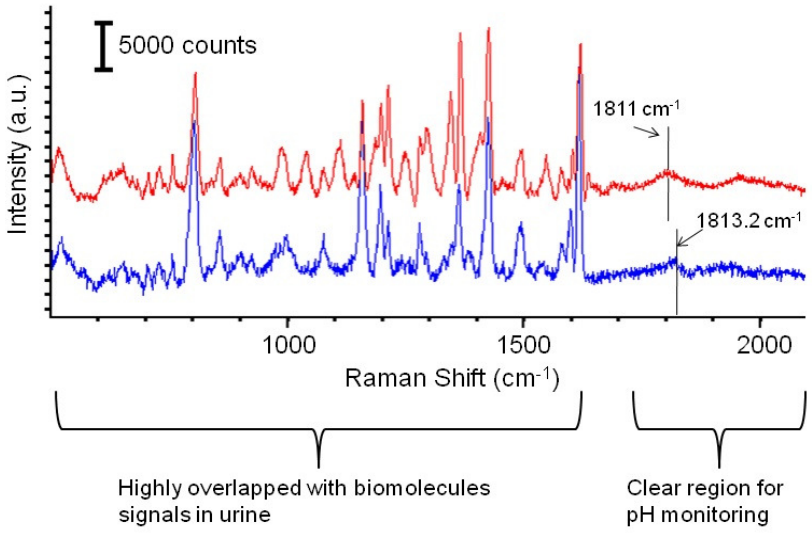
5000 counts
Intensity (a.u.)
1811 cm-1
1813.2 cm-1
1000
1500
2000
Raman Shift (cm-1)
Highly overlapped with biomolecules signals in urine
Clear region for pH monitoring

(A)

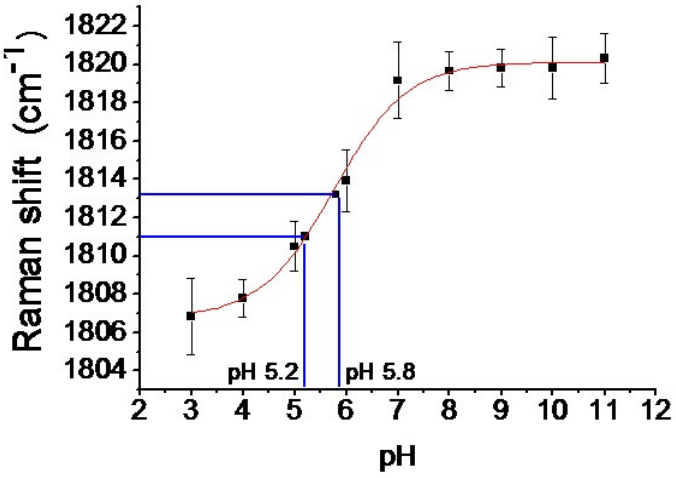
Raman shift (cm-1)
1822
1820
1818
1816
1814
1812
1810
1808
1806
1804
pH 5.2
pH 5.8
2 3 4 5 6 7 8 9 10 11 12
pH

(B)